

## Preparation of Modified Sulfonated Poly(styrene divinybenzene) with Polyaniline as a New Polymer Electrolyte Membrane for Direct Methanol Fuel Cell

Valiollah Mandanipour<sup>1</sup>, Meissam Noroozifar<sup>1,\*</sup>, Ali Reza Modarresi-Alam<sup>2</sup>

<sup>1</sup> Department of Applied Chemistry, University of Sistan and Baluchestan, Zahedan, P.O. Box 98155-674, Iran

<sup>2</sup> Department of Chemistry, polymer research laboratory, University of Sistan and Baluchestan, Zahedan, Iran

\*E-mail: [mnoroozifar@chem.usb.ac.ir](mailto:mnoroozifar@chem.usb.ac.ir)

Received: 12 February 2016 / Accepted: 4 April 2016 / Published: 4 May 2016

---

A new modified proton exchange membrane (PEM) has been prepared with polyaniline (PANI)-sulfonated poly(styrene divinybenzene) resin (SPSD)-polyethylene (PE). The proposed polymer electrolyte membranes (PEM), PANI-SPSD-PE were prepared by blending different ratios of PANI (1-5%) with SPSP-PE and characterized with FT-IR, TGA/DSC and SEM. Different properties of PMEs such as; water uptake, resistance and, conductivity as well as methanol permeability were measured to evaluate its performance in a direct methanol fuel cell (DMFC). The on-set degradation temperature of the SPSP is above 120°C. The ionic conductivity and permeability of the membrane for methanol were increased with increasing of PANI (%) in the membrane and temperature without an extra humidity supply. Finally, a DMFC was designed and assembled with the suggested PANI-SPSD-PE membrane.

---

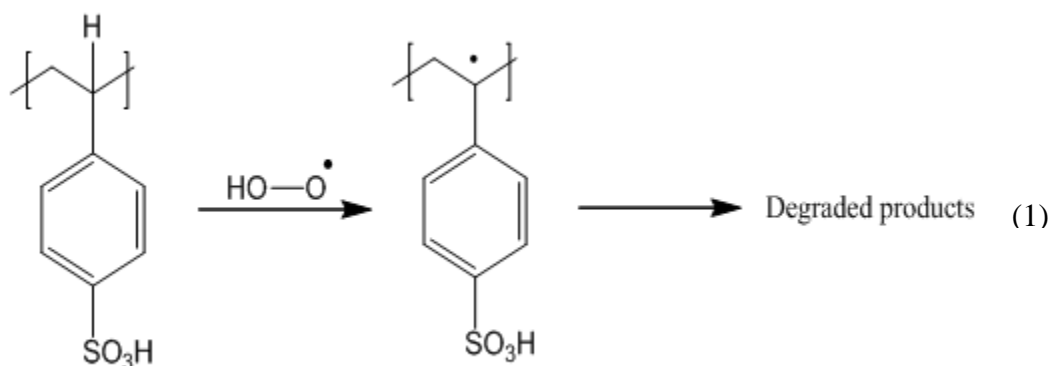
**Keywords:** Polyaniline, Sulfonated poly(styrene divinybenzene), PEM, DMFC, Polymer composites.

### 1. INTRODUCTION

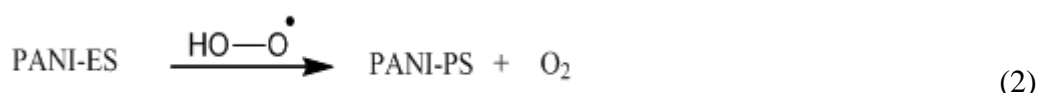
A fuel cell (FC) is a quiet electrochemical device that converts the chemical reaction energy of a fuel such as H<sub>2</sub>, methanol and ethanol into electric power and heat energy [1]. Among them, the DMFC is a type of FC that methanol solution was used as fuel and can be use for portable applications such as; cell phones and laptops [2-5]. In the DMFCs do not require fuel storage and are therefore easy

to handle [6]. The use of PEMFC is the most suitable for automotive application because of low operating temperature, fast start-up procedure, and good dynamic performance [7].

The Nafion<sup>®</sup> membrane is a standard, famous and most popular PEM that has been successfully commercialized for use in FCs. This PEM has high conductivity, excellent chemical stability, high mechanical properties, flexibility, and long lifetime [8-10]. However, PEMFC based on Nafion technology can generally be operated at below 100 °C with high humidity supply due to the decrease of the proton conductivity derived from the water evaporation above its boiling point [11]. Indeed, this membrane has limited application due to low ionic conductivity at temperatures > 80 °C, expensive and high methanol permeability. Many studies have been focused on developing new materials such as sulfonated poly(styrene divinylbenzene), (SPSD) for PEM. However, the lifetime of SPSD as PEM was limited due to the degradation of some peroxide intermediates from oxygen reduction in the cathode side of the FC. The resulted radicals from cathodic side of FC have very strong oxidative capability for chemical attack of the tertiary hydrogen at the  $\alpha$ -carbon of the SPSD (see eq. 1). One of the ways of preventing of degradation is use of SPSD-Nafion composite membrane. Since, Nafion is expensive, a simple and cheap method for barricade of the SPSD oxidation degradation is very necessary.

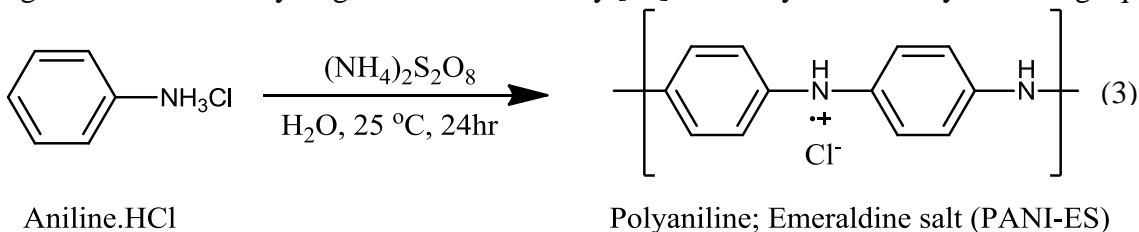


Also, there are a few studies such as poly(5-vinyl tetrazole) and sulfonated polystyrene [11], poly(arylene ether ketone sulfone) [12], poly(arylene ether sulfone) [13], polystyrene-block-poly(ethylene-ran-butylene)-block-polystyrene [14], polybenzimidazoles [15], sulfonated polystyrene/acrylate [16], polyvinylidene fluoride [17], polyamide with bi-functional sulfonimide bridges [18] and sulfonated polybenzimidazole [19] for prevent of the oxidation degradation in PEMs. In other hand, cheap conducting polymers such as polypyrrole (Ppy) and polyaniline (PANI) are good choice for this goal because of their ease of preparation and stability. In fact, PANI and Ppy can be easily synthesized with chemical method by adding an oxidant such as  $\text{Fe}(\text{Cl})_3$  or  $(\text{NH}_4)_2\text{S}_2\text{O}_8$  or electrochemical method by applying an oxidative potential to the monomer solution. PANI has been characterized as a radical scavenger by following equation [20-23];



The conductive PANI can neutralize free radicals by donating electrons and thereby changing their oxidation state from Emeraldine to Pernigraniline. Furthermore, PANI was used as potential

reinforcing and radical scavenging agent for molecular weight polyethylene [24] and SPSD. Also, using PANI is facilitated proton transfer in composite membrane via the conjugated bands [25], to reduce methanol crossover in DMFC application and lead to a very transport of inorganic ions without increasing the resistance to hydrogen ions conductivity [26]. PANI synthesized by following equation;



This polymer has been used for preventing of degradation of SPSD in a SPSD composite membrane.

In this work, a new PEM, polyaniline- sulfonated poly(styrene divinylbenzene)-polyethylene (PANI- SPSD -PE) was prepared and characterized with different techniques. A DMFC was designed and assembled with the suggested PANI- SPSD-PE membrane. The diagram of MEA in the proposed DMFC and half reactions have been summarized in Fig. 1. Based on the Fig. 1, the methanol splits catalytically into protons and electrons in the anode side by the following equation 4. The proton ions, H<sup>+</sup>, permeate through the PEM from anodic side to the cathodic side and the electrons travel along an external load circuit to the cathode side and creating the current output of the fuel cell. The oxygen in cathodic side of MEA react with the H<sup>+</sup> permeating through the PEM to form water molecules according to reaction (5) [27-29].

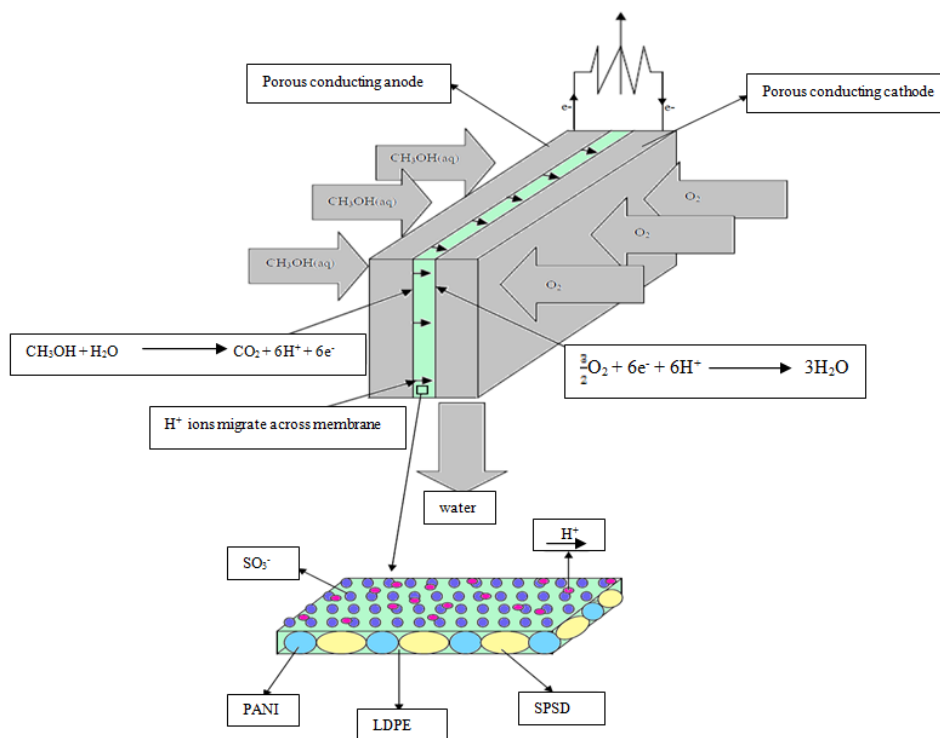
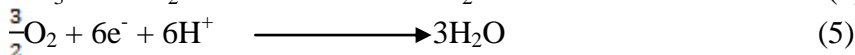
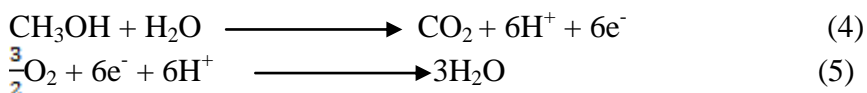


Figure 1. Diagram of MEA in proposed DMFC.

Several parameters, such as the water content, proton conductivity of the membranes, methanol permeability of the membranes and the selectivity factor of the membranes were tested. The optimum membrane was investigated in stack and assembled DMFC and the fuel cell polarization curves were plotted for the mentioned DMFC.

## 2. EXPERIMENTAL

### 2.1 Chemicals

All materials and reagents such as Methanol,  $\text{H}_2\text{PtCl}_6$ , aniline, p-Xylene,  $\text{NaBH}_4$  and SPSD with surface area =  $53 \text{ m}^2 \text{ g}^{-1}$ , average pore diameter  $300 \text{ \AA}$ , resin capacity  $4.7 \text{ eq L}^{-1}$  were purchased from Merck, and used without further purification. Multiwalled carbon nanotubes with OD = 20-30 nm were purchased from Aldrich. Chitosan with molecular weight, 400,000 Da, was purchased from Fluka. Linear low density polyethylene (LDPE) with density  $0.92 \text{ g cm}^3$ , surface hardness SD48, tensile strength 20 Mpa, linear expansion  $20 \times 10^{-5} \text{ }^\circ\text{C}$ , water adsorption 0.01 %, volume resistivity  $10^{16} \text{ } \Omega \cdot \text{cm}$  and melting temperature range  $120\text{-}160 \text{ }^\circ\text{C}$  was purchased from Bandar Imam Petrochemistry. In order to prepare nanosized SPSD, a PM100, RETSCH ball mill instrument was used for 3 h at 500 rpm.

### 2.2 Instrumentation

A JASCO-460 Fourier transform infrared (FT-IR) spectrometer was used for FT-IR spectra of the materials and membranes. A MIRA II LMU (Tescan) scanning electron microscope (SEM) instrument was used for the surface morphology and the status of the samples with a scanning electron microscopy at 15kV. A simultaneous thermal analysis, Mettler Toledo was used for TGA/DSC studies at a flow rate of  $50 \text{ ml min}^{-1}$  under a  $\text{N}_2$  atmosphere and heating rate of  $10 \text{ K min}^{-1}$ .

### 2.3 Preparation of PANI

2.59g aniline hydrochloride was dissolved in a volumetric flask to 50 ml with double distilled water (DDW). An ammonium peroxydisulfate solution was prepared by dissolving of 5.71g in 50 ml DDW. Both solution were kept for 1 h at room temperature (RT), about  $25 \text{ }^\circ\text{C}$ , then mixed in a beaker, briefly stirred, and left to rest in order to polymerize. After one day, the PANI precipitate was collected on a filter, washed with four 100 ml portions of 0.2 M HCl, and four 100 ml portions of acetone. Additional polymerization was carried out in an ice bath at  $0\text{-}2 \text{ }^\circ\text{C}$  [27]. Polyaniline (emeraldine) hydrochloride powder was dried in air and then in an oven at  $60 \text{ }^\circ\text{C}$  [30].

#### 2.4. Preparation of polymer membranes

At first, 1 g of LDPE was dissolved in 25 ml p-Xylene and stirred at 300 rpm for 1.0 h at 100 °C to form a homogeneous solution and then 1 g of milled SPSD with different amounts of PANI, 0.0204 (1%), 0.0512 (2.5 %) and 0.102 (5%) g, was mixed and dissolved in p-Xylene to give a black polymer solution. The solutions were cast on glass plates and dried at 45 °C for 24 h and then at 75 °C in a vacuum for 12 h. The membranes were peeled off, and designated as PANI- SPSD -PE.

#### 2.5. Fuel cell operation

A commercial fuel cell with same characteristics of our previous work was used in this research [31]. In this work an ink catalyst including of PtNPs (4.0 mg.cm<sup>-2</sup>)-CNTs (0.6 mg.cm<sup>-2</sup>) onto a commercial carbon cloth-diffusion layer (4.0PtNPs-0.6CNT/CC-DL) was used as anodic catalyst. The proposed PEM was used between cathode and anode of membrane electrode assembly (MEA).

#### 2.6. Evaluation of membrane properties

The performance of the proposed PEM in the presence of PANI, as a proton exchange membrane component and different properties of PEM such as; water uptake rate, water uptake rate, methanol permeability and selectivity factor had major effects and must be measured.

The water uptake was calculated with the following equation [32]:

$$\text{Water uptake (\%)} = \frac{W_{\text{wet}} - W_{\text{dry}}}{W_{\text{dry}}} \times 100 \quad (6)$$

where  $W_{\text{wet}}$  and  $W_{\text{dry}}$  are wetted and dried membrane weights, previously. The membrane was first immersed in DDW for 24 h and then, the membrane was weighted quickly after removing the surface water to determine the wetted membrane weight ( $W_{\text{wet}}$ ). The dry membrane weight ( $W_{\text{dry}}$ ) was determined after drying the membrane at 373 K for 2 h. The resistance was calculated with the equation 7 as follow [33];

$$\sigma = \frac{L}{RWd} \quad (7)$$

In this equation,  $R(S^{-1})$ ,  $L(\text{cm})$ ,  $W(\text{cm})$  and  $d(\text{cm})$  are the membrane resistance, the distance between potential-sensing electrodes, the width and thickness of the membrane, respectively.

The membrane permeability was calculated with the following equation [33]:

$$P = \frac{1}{C_A} \left( \frac{\Delta C_{B(t)}}{\Delta t} \right) \left( \frac{LV_B}{A} \right) \quad (8)$$

where  $P (\text{cm}^2 \text{ s}^{-1})$ ,  $C_A (\text{mol L}^{-1})$ ,  $DC_{B(t)}/\Delta t (\text{mol L}^{-1} \text{ s})$ ,  $V_B(\text{cm}^3)$ ,  $A(\text{cm}^2)$  and  $L(\text{cm})$  are the methanol diffusion permeability of the membrane, the concentration of methanol in cell A, the slope of the molar concentration variation of methanol in cell B as a function of time, the volume of each diffusion reservoir and the membrane area and is the thickness of the membrane, respectively. The methanol permeability through the membrane was measured using a custom-built two-compartment diffusion cell. The membrane was clamped vertically between two glass compartments; each compartment contained a magnetic stirring bar for solution agitation. The feed compartment was filled with 5 M methanol, and the receiving chamber contained deionized water. The methanol concentration

of the solution in the receiving compartment was measured with a SAMA500 Electroanalyser [34]. Finally, the selectivity factor (the ratio of the proton conductivity ( $\sigma$ ) to the methanol permeability ( $p$ )) was determined with the equation 9;

$$\text{Selectivity} = \frac{\sigma}{p} \quad (9)$$

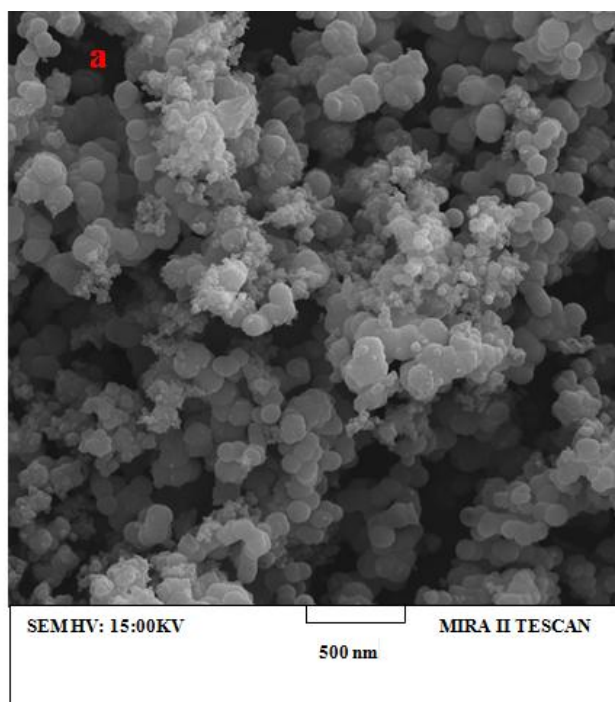
### 3. RESULTS AND DISCUSSION

#### 3.1. SEM characterization

A camera picture of PANI-SPSD-PE has been shown in Fig. 2. The membrane's color is dark green.



**Figure 2.** A camera picture of PANI-SPSD-PE membrane.



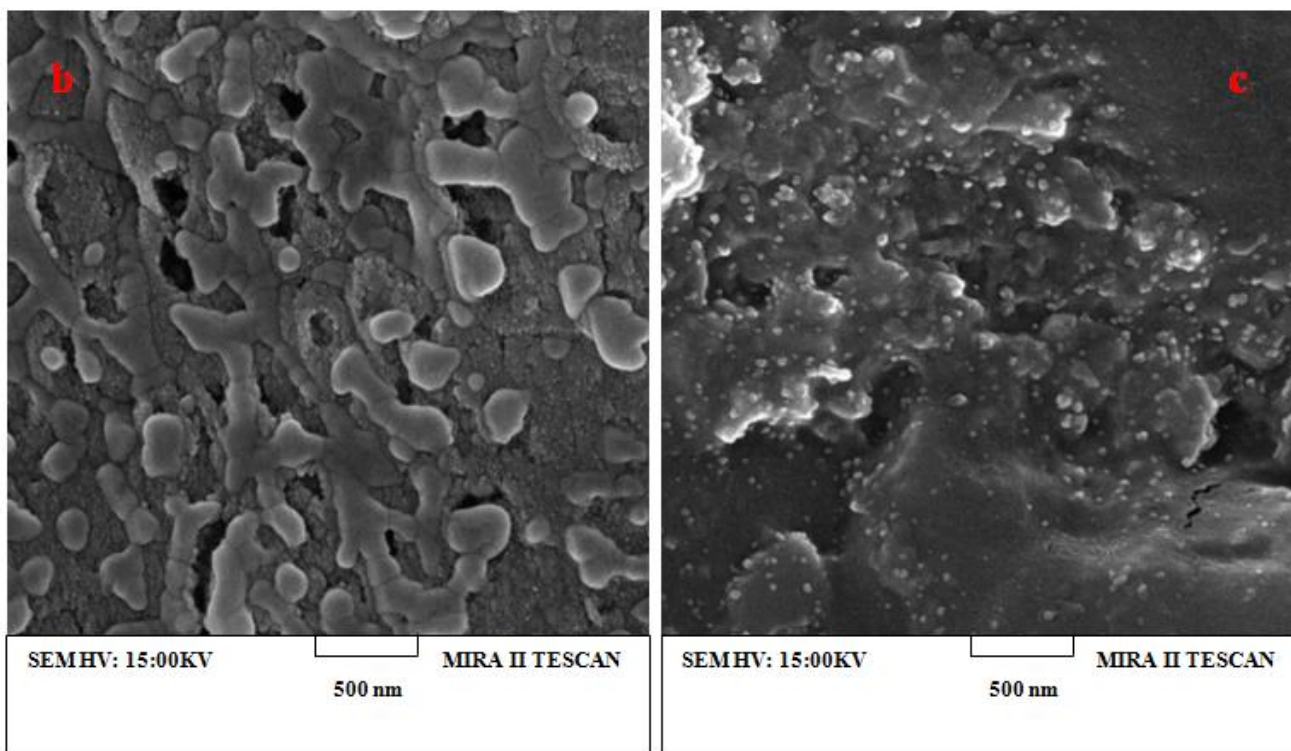


**Figure 3.** SEM images for (a) PANI, (b) SPSD-PE membrane, (c) PANI- SPSD-PE membrane.

SEM provided information about the morphology of the membrane. The SEM measurements were used to characterize the structure of the membrane. Fig. 3 shows the surface micrographs of the PANI, SPSD -PE and PANI- SPSD -PE composite membranes.

The SEM images of the nanoparticles of polyaniline (emeraldine) hydrochloride have been shown in Figure 3a. The images clearly depict the uniform solid nanospheres and their mean diameters are in the size range of 40-100 nm. Fig. 3c show that the hybrid PANI (5%)-SPSD-PE membrane had a finer structure compared to the SPSD -PE membrane (see Fig. 3b), suggesting that the synthesized films were homogeneous and hence formed a more dense membrane. These graphs illustrate that using PANI promotes the formation of small pores in the MEA.

### 3.2. FT-IR characterization

FT-IR important bands of the PANI, PANI (1%)- SPSD -PE, SPSD, PANI (2.5%)- SPSD -PE, PANI(5%)- SPSD -PE and PE are presented in Table 1. The main bands of polyethylene in the IR region are:  $\text{CH}_2$  asymmetric strong stretching in  $2919\text{ cm}^{-1}$ ,  $\text{CH}_2$  symmetric strong stretching in  $2851\text{ cm}^{-1}$ , bending strong deformation in  $1473$  and  $1463\text{ cm}^{-1}$ , wagging medium deformation in  $1366$  and  $1351\text{ cm}^{-1}$ , twisting weak deformation in  $1306\text{ cm}^{-1}$ , wagging very weak deformation in  $1176\text{ cm}^{-1}$  and rocking medium deformation in  $731\text{--}720\text{ cm}^{-1}$ . The FT-IR important bands of the emeraldine salt form of polyaniline shows bands at  $1557\text{ cm}^{-1}$  and at  $1480\text{ cm}^{-1}$  which are characteristic of quinoid and benzenoid rings, respectively, and their presence shows a prominence in the conducting state of the polymer. The band at  $1140\text{ cm}^{-1}$  is characteristic of the protonated states ( $=^+\text{NH}-$  and/or  $-\text{HN}^{\bullet +}$ ). The

absorption band at  $1302\text{ cm}^{-1}$  arises due to C-N stretch of secondary aromatic amine. The peak at  $803\text{ cm}^{-1}$  has been attributed to the para coupled ring, while the peak at  $879\text{ cm}^{-1}$  represents the deformed vibrational mode of the benzene ring. Table 1 shows the FT-IR important bands of the fresh resin sample cross-linked with PsDv-SO<sub>3</sub>H powders. The bands at  $2925$  and  $2876\text{ cm}^{-1}$  are due to the aliphatic C-H stretching absorbance of methylene and methyne groups in the main chain. SO<sub>2</sub> asymmetric stretching appears at  $1385\text{ cm}^{-1}$ . Strong band at  $1652\text{ cm}^{-1}$  indicates an aromatic C=C bond. The four sharp peaks at  $1009\text{ cm}^{-1}$ ,  $1039\text{ cm}^{-1}$ ,  $1129\text{ cm}^{-1}$ ,  $1183\text{ cm}^{-1}$  are due to SO<sub>3</sub> symmetric stretching. The peaks at around  $1619\text{ cm}^{-1}$  are due to the deformation and skeletal vibrations of C-H in Dv. The bonding of the sulfonic groups to the aromatic ring of the cross-linked PsDv-SO<sub>3</sub>H is found at  $833\text{ cm}^{-1}$  (out of plane deformation bands assigned to substituted aromatic ring  $\gamma$  (Car-H)). The obtained FT-IR spectrum confirms the structure of the cross-linked PsDv-SO<sub>3</sub>H-PE membrane. The strong peak centered at  $3432\text{ cm}^{-1}$  can be attributed to the stretching vibration of the acid O-H groups.

The strong peaks at  $2852\text{ cm}^{-1}$  and  $2921\text{ cm}^{-1}$  correspond to the C-H stretching vibration of CH<sub>2</sub> groups. The medium peak centered at  $1633\text{ cm}^{-1}$  can be attributed to the stretching vibration of the C=C groups of benzenes. The medium peak centered at around  $1469\text{ cm}^{-1}$  can be attributed to the bending vibration of the CH<sub>2</sub> groups and C=C aromatic groups. The four sharp peaks at  $1009\text{ cm}^{-1}$ ,  $1039\text{ cm}^{-1}$ ,  $1128\text{ cm}^{-1}$  and  $1179\text{ cm}^{-1}$  clearly show SO<sub>3</sub> symmetric stretching as described above. Table 1 shows the FT-IR important bands of the composite materials prepared by reinforcement of the membrane, i.e. adding polyaniline to SPSD-PE in different compositions such as 0.02, 0.05 and 0.1 gr (1, 2.5 and 5 %). The FT-IR studies reveal the formation of composite materials and help qualitatively obtain their compositions. In case of composites, the out of plane H deformation, i.e. substituted aromatic ring was observed at  $833\text{ cm}^{-1}$ . The bands at around  $1472\text{ cm}^{-1}$  and  $1617\text{ cm}^{-1}$  correspond to C=C vibrations of benzenoid and quinoid rings in the PANI emeraldine salt chain, respectively. The intensity of these bands goes on increasing with the increase in PANI content. The strong peaks at  $2852\text{ cm}^{-1}$  and  $2921\text{ cm}^{-1}$  correspond to the C-H stretching vibration of the CH<sub>2</sub> groups. The peak at  $1000\text{--}1180\text{ cm}^{-1}$  corresponds to the sulfonic acid group in all these compositions, i.e. the symmetric-SO<sub>3</sub> stretching described above. The intensity of these bands goes on decreasing with the increase in PANI content. The characteristic bands of the three components SPSD, PE and PANI confirm the presence of three phases in the composite materials, but all these bands show a systematic shifting that indicates the existence of significant interaction between PANI and PSSA in the composite materials [34].

**Table 1.** FT-IR important bands for SPSD, PE, PANI and SPSD-PE-PANI membrane

Samples	Important Bands (cm <sup>-1</sup> )
SPSD	3417, 2925, 2876, 1652, 1619, 1385, 1183, 1129, 1039, 1009, 833
PE	2921, 2851, 1471, 1366, 1351, 1176, 1306, 1083, 731, 719
PANI	3413, 1557, 1480, 1302, 1140, 879, 803
SPSD-PE-PANI	3416, 2921, 2852, 1617, 1471, 1385, 1179, 1128, 1039, 1009, 833, 776, 718

3.3. Membrane properties measurements

Fig 4a was shown the water content of the entire nanocomposite membranes equilibrated with 100% relative humidity air at 25 °C and immersed in liquid water at 25 °C. As shown in Fig 4a, the water content was high in the nanocomposite with higher PANI values (5% PANI) membrane (57.22%) than in membrane with lower PANI values (43.99% for membrane with (2.5%PANI) and 32.41% for membrane with(1% PANI) [26]. The nanocomposite membranes with more PANI had a higher water uptake rate compared with the nanocomposite membranes with less PANI. The water content is important for the ion transportation in the membrane, so a higher water uptake rate may improve the performance of a fuel cell.

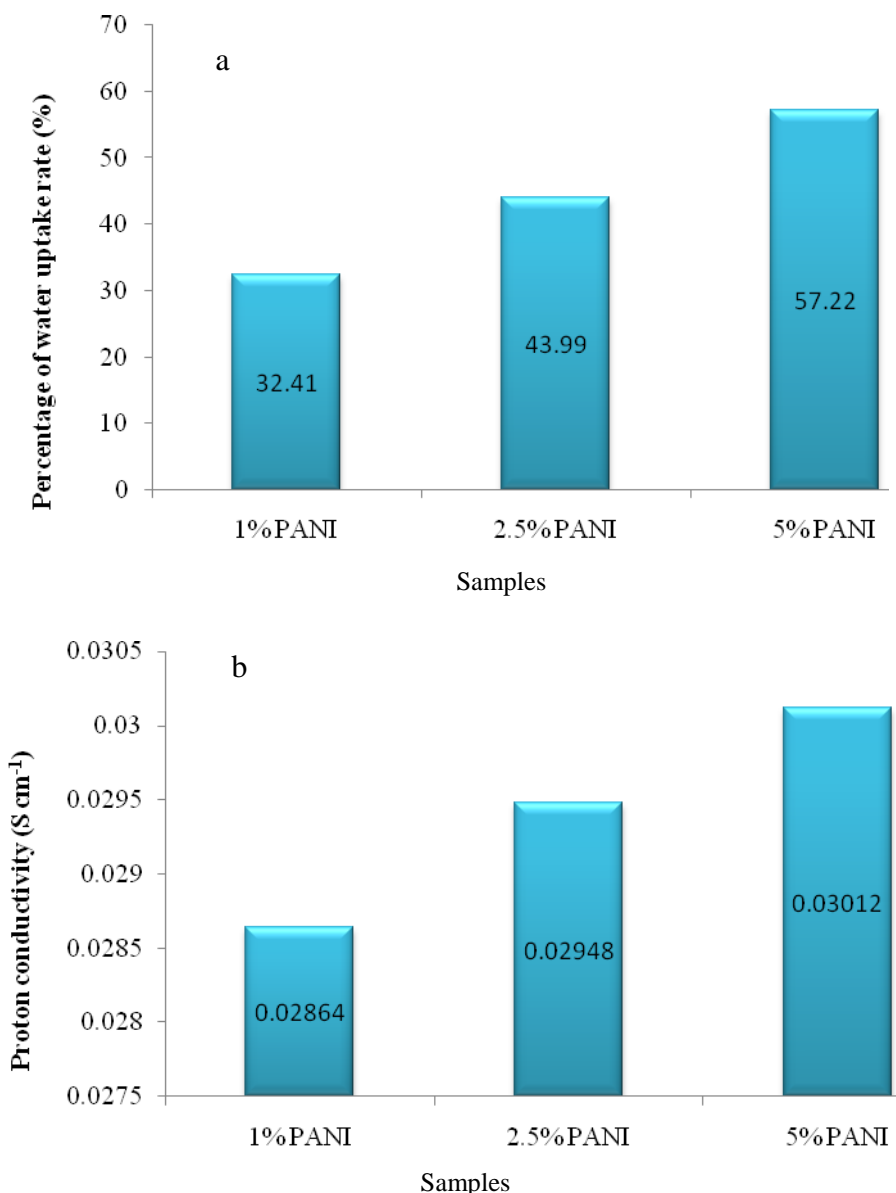


**Figure 4.** (a) Water uptake rate of different types of membrane and (b) Proton conductivity of wet samples of membranes at RT.

The proton conductivity of the membrane samples were measured at RT and 100% relative humidity. We also tested the membrane with water for one full day. Figure 4b show the proton conductivity of the nanocomposite membranes. Based on the results, the membrane with high PANI (%) had relatively higher proton conductivity compared to the membrane with less PANI (%).

The methanol permeability of the membranes was measured at RT using a 5 M methanol solution and the results were shown in Table 2. Based on the results, the methanol permeability in the nanocomposite membrane with less PANI (%) was relatively lower than that of the nanocomposite membrane with high PANI (%) and the selectivity factor for the nanocomposite membrane with high PANI (%) was relatively better than the nanocomposite membrane with less PANI. Also, the results of the selectivity factor were shown in Table 2. A membrane with lower methanol permeability is advantageous for DMFC usage and it is very important because increasing the proton conductivity and decreasing the methanol permeability is the goal DMFC membranes. The selectivity factor, proton conductivity and methanol permeability, can be treated as a guide for developing better DMFC membrane characteristics [35]. The higher selectivity factor contributes to better DMFC performance.

**Table 2.** Proton conductivity, methanol permeability and selectivity factor of all the membranes.

Membrane with different amount of PANI (%)	Proton conductivity $\sigma$ (S.cm)	Methanol permeability P (cm <sup>2</sup> .s <sup>-1</sup> )	Selectivity factor $\sigma / P$ (S.s.cm <sup>-3</sup> )
1.0	$2.90 \times 10^{-2}$	$6.96 \times 10^{-7}$	$4.11 \times 10^4$
2.5	$2.95 \times 10^{-2}$	$7.02 \times 10^{-7}$	$4.20 \times 10^4$
5.0	$3.01 \times 10^{-2}$	$7.05 \times 10^{-7}$	$4.27 \times 10^4$

### 3.4. Thermal analysis techniques (TG-DSC) characterizations

Fig. 5 shows the TGA and DSC curves for SPSD -PE, PANI (1%)-SPSD-PE, PANI (2.5%)-SPSD-PE and PANI (5%)-SPSD-PE. The SPSD -PE and PANI (1%)- SPSD -PE membranes exhibit eight weight-loss zone degradation (Fig. 5a and b).The parameters associated with this weight-loss regions are similar to those observed in the TGA and DSC of SPSD -PE and PANI (1%)- SPSD -PE. However, for the two later membranes, PANI (2.5%)- SPSD -PE and PANI (5%)- SPSD -PE, exhibit three weight zone degradations. Based on Fig 5a-d, the first weight-loss region is centered around 105–140°C for all samples. It is well known that membranes strongly absorb water, so this weight-loss may be attributed to the loss of the absorbed water. The second main weight-loss regions are located around 421-480, 421-480, 400-475 and 425-490 °C for SPSD -PE,PANI (1%)- SPSD -PE, PANI (2.5%)-SPSD -PE and PANI (5%)- SPSD -PE, respectively. Weight losses of 47–57% occur in this region for all samples. This weight-loss zone is associated with the greatest mass loss and is termed, therefore, the main stage. Therefore, this mass loss has been attributed to the complete thermo-degradation of the skeletal chain structure of the composite. All samples show a smaller weight loss occurring above 650 °C for SPSD -PE and PANI (1%)- SPSD -PE and above 700 °C for PANI (2.5%)- SPSD -PE and PANI (5%)- SPSD -PE which can be due to the elimination of organic moieties. The weight loss

within the range 650–800 °C is due to the decomposition of polystyrene-divinylbenzene and PANI [36, 37]. From Fig. 5c and d, it is found that the offset decomposition temperatures of PANI (2.5%)-SPSD-PE, PANI (5%)-SPSD-PE composites were higher those that of SPSPD-PE and PANI (1%)-SPSD-PE and shifted towards the higher temperature range as the content of nanostructured PANI increased whereas the onset value decreases because the small particles changed the rate of reaction and hence the shape of the TGA curves.

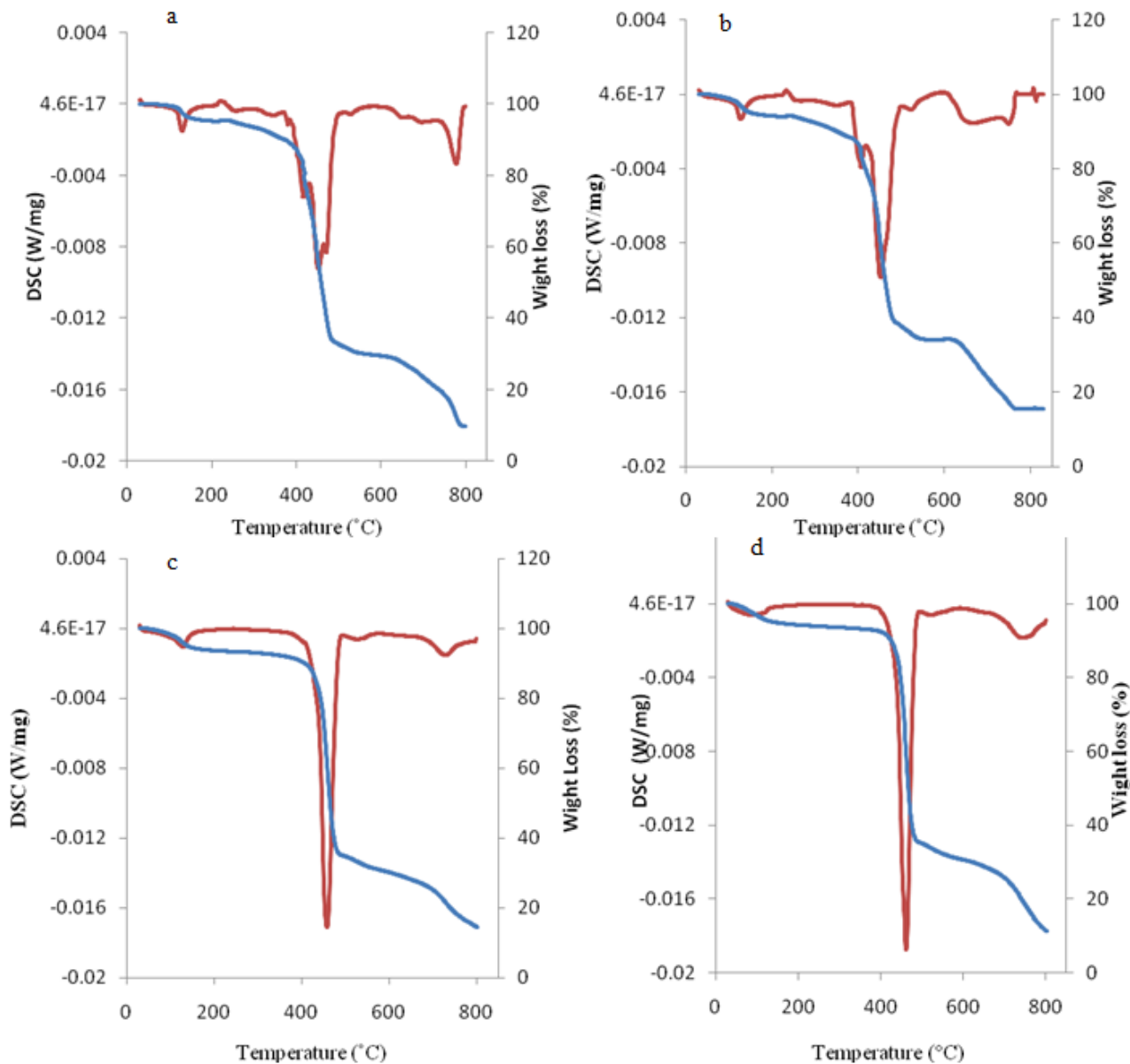


**Figure 5.** TGA (—) and DSC(—) analysis of all of the membranes in a temperature range from 30 to 800 °C for (a) SPSPD-PE, (b) PANI (1%)-SPSPD-PE, (c) PANI (2.5%)-SPSPD-PE and (d) PANI (5%)-SPSPD-PE.

Table 3 was shown a comparison study for proposed membrane with some membrane in literatures. Based on the results, the degradation temperature of the proposed membrane is higher than other membranes.

**Table 3.** Degradation temperature of different membrane with proposed membrane.

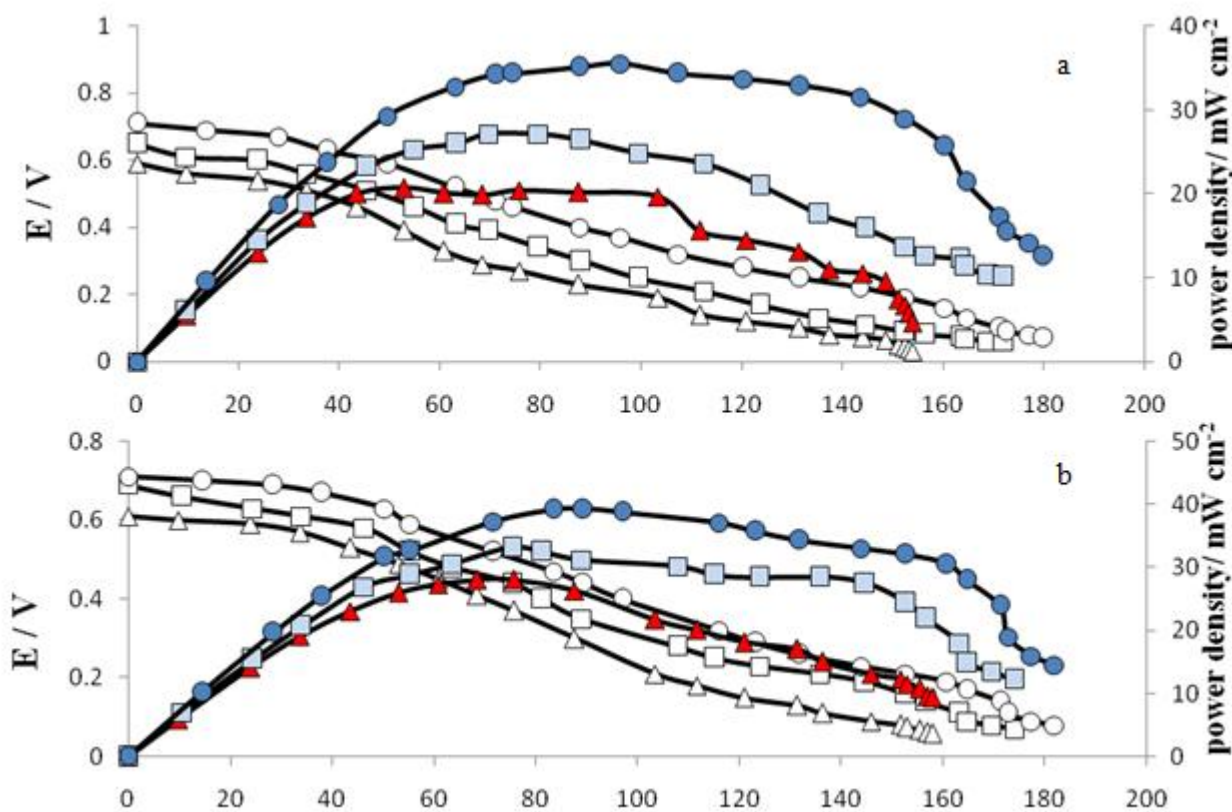
Membranes	Degradation Temperature / ° C	Ref.
SEBS <sup>a</sup>	430	[10]
PVT <sup>b</sup>	400	[11]
Si-sPS/A <sup>c</sup>	350	[16]
Na-PBI-ZP <sup>d</sup>	450	[33]
PANI- SPSD -PE	460	This work

<sup>a</sup>polyStyrene-block-poly(Ethylene-ran-butylene)-Block-Polystyrene, <sup>b</sup> Ppoly(5-Vinyl Tetrazole), <sup>c</sup>Silicon-containing Sulfonated Polystyrene/Acrylate, <sup>d</sup>polybenzimidazole-zirconium phosphate (ZP)

### 3.5. Single cell performances

For understand the performance of the proposed PME, single cell test with proposed PANI-SPSD -PE membrane were carried out for CH<sub>3</sub>OH as fuel and O<sub>2</sub> as oxidant. For increasing the performance and the efficiency of the electrochemical reaction of the fuel cell, different parameters such as PANI (%) in membrane, methanol concentration in fuel side and fuel cell temperature as well as fuel flow rate must be optimized.

The effect of PANI (%) in the proposed membrane on the performance of the fuel cell were tested for various PANI (%) from 1.0 (%) to 5.0 (%) while keeping [methanol] constant at 2M with a flow rate of 1.6 ml min<sup>-1</sup> and [P<sub>O<sub>2</sub>] 2 bar at 80°C. The results have been shown in Fig.6a.</sub>



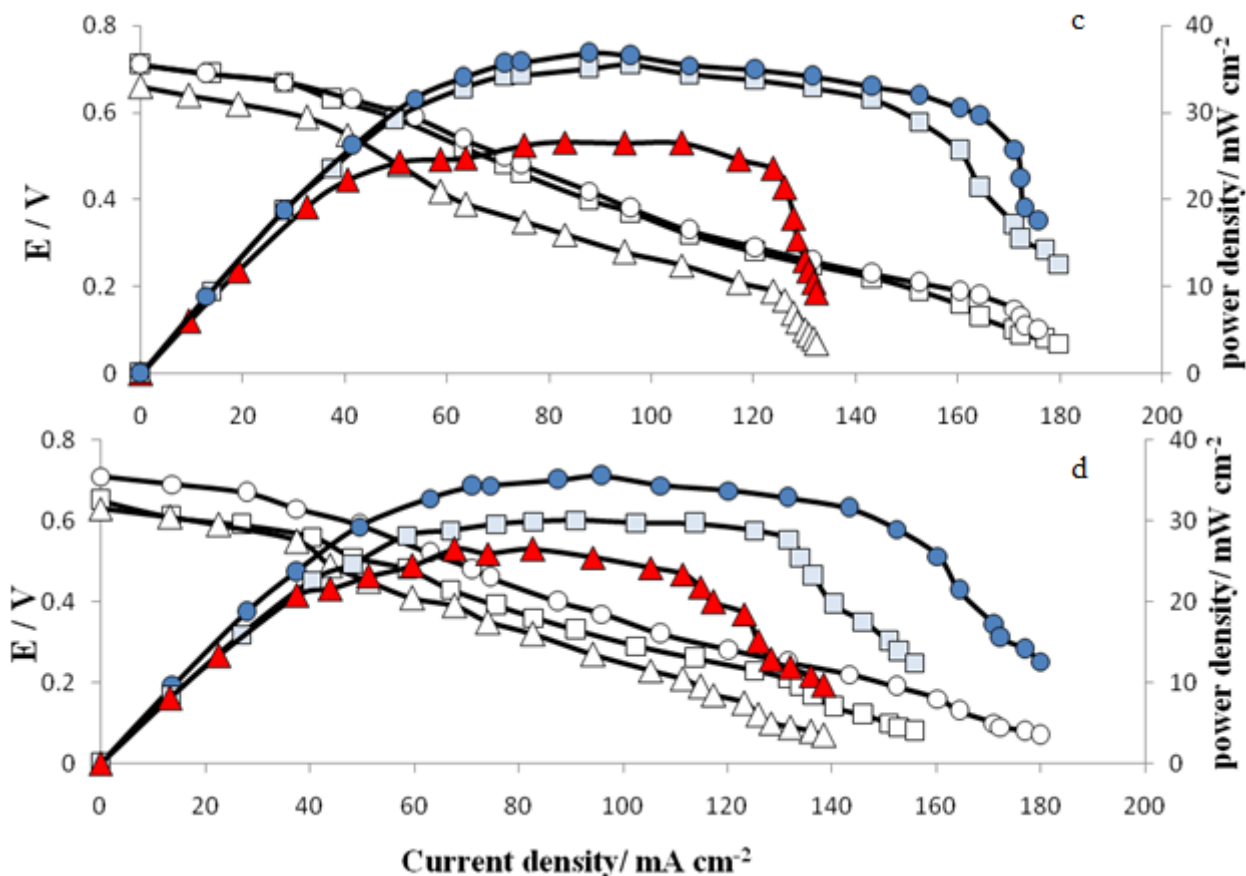


**Figure 6.** Electrical performances (Cell voltage against current density and power density against current density) of a 5 cm<sup>2</sup> DMFC (a) with PANI-SPSD-PE membrane with different PANI (%) (▲) 1, (■) 2.5 and (●) 5.0 (%),  $P_{O_2} = 2$  bar; [Methanol] = 2.0 M; flow rate = 1.6 ml.min<sup>-1</sup> Temperature = 80 °C (b) with different concentration of methanol (▲) 1.0, (●) 2.0 and (■) 3.0 (M)  $P_{O_2} = 2$  bar; [Methanol] = 2.0 M; flow rate = 1.6 ml.min<sup>-1</sup>, Temperature = 80 °C, PANI-SPSD -PE membrane with 5.0 (%) PANI (c) with different temperature (▲) 70.0, (■) 80.0 and (●) 90.0 (°C),  $P_{O_2} = 2$  bar; [Methanol] = 2.0 M; flow rate = 1.6 ml.min<sup>-1</sup>, PANI-SPSD -PE membrane with 5.0 (%) PANI and (d) with different fuel flow rates (▲) 1.0, (●) 1.6 and (■) 2.3 (ml min<sup>-1</sup>) Temperature = 80 °C,  $P_{O_2} = 2$  bar; [Methanol] = 2.0 M, PANI-SPSD -PE membrane with 5.0 (%) PANI.

Based on the results, the maximum power densities of the single cells were obtained as 17, 25 and 35 mWcm<sup>-2</sup> for membranes with 1, 2.5 and 5 % PANI. Furthermore, the OCV of single cells were obtained as 0.58, 0.65 and 0.7 V for membranes with 1, 2.5 and 5 % PANI, respectively. A membrane with 5 % PANI was chosen as optimum for the PANI-SPSD-PE membrane. Fig. 6b shows the results for the effect of methanol concentration in the proposed DMFC in the range from 1 to 3 M methanol. Based on Fig. 6b, the amount of OCV increased with an increase of the methanol concentration from 1 to 2 M and then decreased with increasing the concentration to 3M. Based on these results, a 2 M methanol concentration was chosen as optimum. The effect of temperature on the performance of the fuel cell were tested for temperature from 70 to 90 °C and the results have been shown in Fig 6c. Based on the results, the maximum power densities were obtained at 80 and 90 °C and 80 °C was chosen as optimum for the DMFC temperature. Finally, the effect of fuel flow rates has been studied

for the various flow rates: 1.0, 1.6 and 2.3ml min<sup>-1</sup>.The results have been shown in Fig. 6d. Based on the results, a flow rate 1.6 mL min<sup>-1</sup> was-chosen as optimum fuel flow rate.

**Table 4.** Comparison the proposed DMFC with PANI- SPSD -PE membrane with other DMFCs with different membranes.

Membrane	Memb rane size / cm <sup>2</sup>	Anode loading/ mg.cm <sup>-2</sup>	Cathode loading/ mg.cm <sup>-2</sup>	Tempera ture/ °C	Methanol concentrat ion/ M	Power Density/ mW.cm <sup>-2</sup>	Ref.
Nafion 117	4	8- Pt/Ru	8- Pt	RT	5	8.6	[33]
Nafion-ZP <sup>a</sup>	3	1-1.25- Pt/Ru	5- Pt	RT	1	6-8	[33]
Nafion- Mordenite SDMFC <sup>b</sup>	4.5	1- Pt/Ru	1-60% Pt/C	70	2	37	[38]
Nafion- Polyaniline - Silica	4	3- 40% Pt/20% Ru/C	1.75- 40% Pt/C	60	1	9.4	[39]
Nafion- Polyaniline - Silica	5	4- 80 wt% Pt/Ru on carbon	4- Pt	40	2	8	[40]
PANI (1%)- SPSD -PE	5	4.0-PtNPs-0.6- CNT/CC-DL	2- Pt	80	2	17	This wor k
PANI (2.5%)- SPSD -PE	5	4.0-PtNPs-0.6- CNT/CC-DL	2- Pt	80	2	25	
PANI (5%)- SPSD -PE	5	4.0-PtNPs-0.6- CNT/CC-DL	2- Pt	80	2	35	

<sup>a</sup> zirconium phosphate (ZP), <sup>b</sup> special-shaped direct methanol fuel cell.

#### 4. CONCLUSION

For the first time, SPSD composites with different weight percentages of PANI in PE were synthesized by a simple method and the new membranes were characterized by FTIR, SEM and TGA/DSC. The conductivity of membranes was relatively increased with increasing of weight percent of PANI in SPSD -PE composites and fuel cell's temperatures. It was observed from the electrical conductivity studies that the 5 wt % of PANI in the polymer matrix shows an enhancement of conductivity of the conducting polyaniline and their values are found to be in the semiconducting range. The TGA-DSC studies confirmed the increased thermal stability of composites, as the content of nanostructured PANI increased, which could be attributed to the retardation effect of PANI as barriers for the degradation of SPSD -PE composites. Table 4 was shown a comparison study for proposed DMFC with some FC in literatures. In comparison with other FCs that reported for the DMFC, this FC has better and satisfactory results.

## References

1. S.M.C. Ang, E.S. Fraga, N.P. Brandon, N.J. Samsatli, D.J.L. Brett, *Int. J. Hydrogen Energy* 36 (2011) 14678.
2. A. Heinzl, V.M. Barragan, *J. Power Sources* 84 (1999) 70.
3. V. Neburchilov, J. Martin, H. Wang, J. Zhang, H. Wang, *J. Power Sources* 169 (2007) 221.
4. K.Y. Cho, J.Y. Eom, H.Y. Jung, N.S. Choi, Y.M. Lee, J.K. Park, J.H. Choi, K.W. Park, Y.E. Sung, *Electrochim. Acta* 50 (2004) 583.
5. P. Dimitrova, K.A. Friedrich, B. Vogt, U. Stimming, *J. Electroanal. Chem.* 532 (2002) 75.
6. A.M. Zainoodin, S.K. Kamarudin, M.S. Masdar, W.R.W. Daud, A.B. Mohamad, J. Sahari, *Appl. Energy* 113(2014) 946.
7. J. Jer-Huan, Y. Wei-Mon, Ch. Han-Chieh, L. Jun-Yi, *Applied Energy*, 142 (2015) 108.
8. C. Perrot, L. Gonon, C. Marestin, G. Gebel, *J. Membr. Sci.*, 379 (2011) 207.
9. Y. Wang, J. Geder, J.M. Schubert, R. Dahl, J. Pasel, R. Peters, *Fuel Process. Technol.*, 95 (2012) 144.
10. X. Wei, M.Z. Yates, *J. Power Sources*, 195 (2010) 736.
11. L. Jinhuan, W. Jianxin, Ch. Xiangqun, L. Zhaoping, Ch. Tian, W. Tangyang, *Solid State Ionics*, 255 (2014) 128.
12. J. Xu, L. Ma, H. Han, H. Ni, Z. Wang, H. Zhang, *Electrochim. Acta*, 146 (2014) 688.
13. D. J. Kim, H. J. Lee, S. Y. Nam, *Int. J. Hydrogen Energy*, 39 (2013) 17524.
14. Q. H. Zeng, Q. L. Liu, I. Broadwell, A. M. Zhu, Y. Xiong, X. P. Tu, *J. Membr. Sci.*, 349 (2010) 237.
15. Q. Li, J. O. Jensen, R. F. Savinell, N. J. Bjerrum, *Prog. Polym. Sci.*, 34 (2009) 449.
16. Sh. Zhong, Xu. Cui, S. Dou, W. Liu, Y. Gao, B. Hong, *Electrochim. Acta*, 55 (2010) 8410.
17. E. F. Abdrashitov, V. Ch. Bokun, D. A. Kritskaya, E. A. Sanginov, A. N. Ponomarev, Y. A. Dobrovolsky, *Solid State Ionics*, 251 (2013) 9.
18. L. Jing, C. Weiwei, Zh. Yunfeng, Ch. Zhangxian, X. Guodong, C. Hansong, *Electrochim. Acta*, 151 (2015) 168.
19. Y. Yan, W. Jiabin, Y. Xiaole, D. Qing, F. Jianhua, J. Kui. *Int. J. Hydrogen Energy*, 39 (2014) 13671.
20. G. Cirillo, F. Iemma, "Antioxidant Polymers: Synthesis, Properties, and Applications", John Wiley & Sons, 2012.
21. Z. D. Zujovic, M. Gizdavic-Nikolaidis, P. A. Kilmartin, J. Travas-Sejdic, R. P. Cooney, G. A. Bowmaker, *Applied Magnetic Resonance*, 28 (2005) 123.
22. J.-Y. Fang, K. C. Fang, C.-P. Hsu, C. H. Chu, J. Liu, and Y.-L. Wang, *ECS Trans.*, 64 (2014) 63.
23. J. Yu, B. Yi, D. Xing, F. Liu, Z. Shao, Y. Fu, H. Zhang, *Phys. Chem. Chem. Phys.*, 5 (2003) 611.
24. F. Addiego, I. Mihai, D. Marti, K. Wang, V. Toniazzo, D. Ruch, *Synthetic Metals*, 198 (2014) 196.
25. J. Yang, P. K. Shen, J. Varcoe, Z. Wei., *J. Power Sources*, 189 (2009) 1016.
26. S. Tan, D. Bélanger, *J. Phys. Chem. B.*, 109 (2005) 23480.
27. M. A. Hassan, S. K. Kamarudin, K. S. Loh, W. R. W. Daud, *Renew. Sust. Energ. Rev.*, 40 (2014) 1060.
28. G. Merle, M. Wessling, K. Nijmeijer, *J. Membr. Sci.*, 377 (2011) 1.
29. A. C. Fărcaș, P. Dobra, *Procedia Technol.*, 12 (2014) 42.
30. J. Stejskal, *Pure appl. chem.*, 74 (2002) 857.
31. Z. Yavari, M. Noroozifar, M. Khorasani-Motlagh, *J. Appl. Electrochem.*, 45 (2015) 439.
32. H. Ahmad, S. K. Kamarudin, U.A. Hasran, W. R.W. Daud, *Int. J. Hydrogen Energy*, 35 (2010) 2160.
33. H. Ahmad, S.K. Kamarudin, U.A. Hasran, W.R.W. Daud, *Int. J. Hydrogen Energy*, 36 (2011) 14668.

34. M. Khorasani-Motlagh, M. Noroozifar, M.-S. Ekrami-Kakhki, *Int. J. Hydrogen Energy*, 36 (2011) 11554.
35. A. K. Mishraa, S. Boseb, T. Kuilab, N. H. Kimc, J. H. Lee, *Prog. Polym. Sci.*, 37 (2012) 842.
36. J. Farmera, B. Duonga, S. Seraphina, S. Shimpaleeb, M.J.M. Rodríguezb, J.W. Van Zee, *J. Power Sources*, 197 (2012) 1.
37. S. Park , B.N. Popov, *Fuel*, 88 (2009) 2068.
38. Ch. Yoonoo, C. P. Dawson, E. P.L. Roberts, S. M. Holmes, *J. Membr. Sci.*, 369 (2011) 367.
39. H-J. Ni, Ch-J. Zhang, Xi-Xi. Wang, Su-Y. Ma, P. Liao, *J Fuel Chem Technol*, 38 (2010) 604.
40. C.Y. Chen, J.I. Garnica-Rodriguez, M.C. Duke, R.F. Dalla Costa, A.L. Dicks, J.C. Diniz da Costa, *J. Power Sources*, 166 (2007) 324.

© 2016 The Authors. Published by ESG ([www.electrochemsci.org](http://www.electrochemsci.org)). This article is an open access article distributed under the terms and conditions of the Creative Commons Attribution license (<http://creativecommons.org/licenses/by/4.0/>).